J Physiol 589.24 (2011) pp 6039–6050

The Journal of Physiology

Regulation of sarcoplasmic reticulum Ca^{2+} leak by cytosolic Ca^{2+} in rabbit ventricular myocytes

Elisa Bovo[1], Stefan R. Mazurek[1], Lothar A. Blatter[2] and Aleksey V. Zima[1]

[1] *Department of Cell and Molecular Physiology, Loyola University Chicago, Stritch School of Medicine, 2160 South First Avenue, Maywood, IL 60153, USA*

[2] *Department of Molecular Biophysics and Physiology, Rush University Medical Centre, 1750 West Harrison Street, Chicago, IL 60612, USA*

Non-technical summary Contraction and relaxation of the heart strongly depend on calcium (Ca^{2+}) stored in the sarcoplasmic reticulum (SR). Ca^{2+} stored within the SR is determined by the balance between Ca^{2+} uptake and Ca^{2+} leak that occurs mainly via Ca^{2+} release channels, called ryanodine receptors (RyRs). Alterations in the RyR activity can lead to enhanced SR Ca^{2+} leak and arrhythmias. Ca^{2+} tightly regulates the RyR activity from both sides of the SR (cytosolic and luminal). In this work, we studied the effects of cytosolic Ca^{2+} on SR Ca^{2+} leak in isolated ventricular myocytes. Elevation of cytosolic Ca^{2+} increased SR Ca^{2+} leak by a direct activation of RyRs. In intact myocytes, at the end of contraction and at the beginning of the relaxation phase, SR Ca^{2+} leak remains relatively constant due to the coordinated regulation of RyRs by cytosolic and luminal Ca^{2+}. Thus, this dual regulation of the RyR contributes to the control of the SR Ca^{2+} content, preventing excessive loss of Ca^{2+} that could lead to pathological conditions such as cardiac arrhythmia.

Abstract Sarcoplasmic reticulum (SR) Ca^{2+} leak determines SR Ca^{2+} content and, therefore, the amplitude of global Ca^{2+} transients in ventricular myocytes. However, it remains unresolved to what extent Ca^{2+} leak can be modulated by cytosolic $[Ca^{2+}]$ ($[Ca^{2+}]_i$). Here, we studied the effects of $[Ca^{2+}]_i$ on SR Ca^{2+} leak in permeabilized rabbit ventricular myocytes. Using confocal microscopy we monitored SR Ca^{2+} leak as the change in $[Ca^{2+}]_{SR}$ (with Fluo-5N) after complete SERCA inhibition with thapsigargin (10 μm). Increasing $[Ca^{2+}]_i$ from 150 to 250 nM significantly increased SR Ca^{2+} leak over the entire range of $[Ca^{2+}]_{SR}$. This increase was associated with an augmentation of both Ca^{2+} spark- and non-spark-mediated Ca^{2+} leak. Further increasing $[Ca^{2+}]_i$ to 350 nM led to rapid $[Ca]^{2+}]_{SR}$ depletion due to the occurrence of Ca^{2+} waves. The augmentation of SR Ca^{2+} leak by high $[Ca^{2+}]_i$ was insensitive to inhibition of Ca^{2+}–calmodulin-dependent protein kinase II. In contrast, lowering $[Ca^{2+}]_i$ to 50 nM markedly decreased SR Ca^{2+} leak rate and nearly abolished Ca^{2+} sparks. When the ryanodine receptor (RyR) was completely inhibited with ruthenium red (50 μM), changes in $[Ca^{2+}]_i$ between 50 and 350 nM did not produce any significant effect on SR Ca^{2+} leak, indicating that $[Ca^{2+}]_i$ alters SR Ca^{2+} leak solely by regulating RyR activity. In summary, $[Ca^{2+}]_i$ in the range of 50–350 nM has a significant effect on SR Ca^{2+} leak rate mainly via direct regulation of RyR activity. As RyR activity depends highly on $[Ca^{2+}]_i$ and $[Ca^{2+}]_{SR}$, SR Ca^{2+} leak remains relatively constant during the declining phase of the Ca^{2+} transient when $[Ca^{2+}]_{SR}$ and $[Ca^{2+}]_i$ change in opposite directions.

(Received 15 June 2011; accepted after revision 5 October 2011; first published online 10 October 2011)

Corresponding author A. V. Zima: Department of Cell and Molecular Physiology, Loyola University Chicago, Stritch School of Medicine, 2160 South First Avenue, Maywood, IL 60153, USA. Email: azima@lumc.edu

Abbreviation AIP, autocamtide 2-related inhibitory peptide; $[Ca^{2+}]_i$, cytosolic free calcium concentration; CaMKII, Ca^{2+}–calmodulin-dependent kinase type II; CICR, Ca^{2+}-induced Ca^{2+} release, ECC, excitation–contraction coupling; FDHM, full duration at half-maximum; FWHM, full width at half-maximum; HF, heart failure; NCX, Na^+–Ca^{2+} exchange; PLB, phospholamban; RuR, ruthenium red; RyR, ryanodine receptor; SERCA, sarcoplasmic/endoplasmic reticulum Ca^{2+}-ATPase; SR, sarcoplasmic reticulum; $[Ca^{2+}]_{SR}$, sarcoplasmic reticulum free calcium concentration; TG, thapsigargin.

DOI: 10.1113/jphysiol.2011.214171

Introduction

During systole, Ca^{2+} influx via L-type Ca^{2+} channels activates ryanodine receptors (RyRs) causing global Ca^{2+} release that initiates contraction in cardiac muscle. This process is known as Ca^{2+}-induced Ca^{2+} release (CICR; Fabiato, 1983). After CICR termination, a large portion of cytosolic Ca^{2+} is pumped back into the sarcoplasmic reticulum (SR) by the Ca^{2+}-ATPase (SERCA) leading to cardiac muscle relaxation. However, RyRs are not continuously closed during diastole and spontaneous openings of RyRs generate substantial SR Ca^{2+} leak. By counterbalancing SR Ca^{2+} uptake, diastolic SR Ca^{2+} leak plays an important role in setting and maintaining the appropriate SR Ca^{2+} load in the healthy heart (Shannon *et al.* 2002; Zima *et al.* 2010). However, during the development of heart failure (HF) RyRs undergo post-translational modifications that ultimately lead to an increase in SR Ca^{2+} leak (Ai *et al.* 2005; Belevych *et al.* 2007; Zima *et al.* 2010). This excessive Ca^{2+} leak has been implicated in reduction of contractile force as well as in cardiac arrhythmias (George, 2008). Although the precise mechanisms of RyR modification during HF remain highly controversial (Bers *et al.* 2003; Lehnart & Marks, 2007), it has been shown that abnormal phosphorylation of RyR either by protein kinase A (PKA; Marx *et al.* 2000) or Ca^{2+}–calmodulin-dependent kinase type II (CaMKII; Ai *et al.* 2005) is involved in the augmentation of SR Ca^{2+} leak. Additionally, oxidation of thiol groups of the RyR can contribute to an alteration of SR Ca^{2+} leak in HF (Terentyev *et al.* 2008). Failing cardiac myocytes also exhibit a slower decay of cytosolic Ca^{2+} transient during excitation–contraction coupling (ECC) (O'Rourke *et al.* 1999; Jiang *et al.* 2002) due, presumably, to down-regulation of SERCA activity and a subsequent impairment of SR Ca^{2+} reuptake (Pieske *et al.* 1995; Pogwizd *et al.* 1999). Additionally, it has been reported that in failing myocytes cytosolic $[Na^+]$ is significantly increased. This can contribute to further slowing of Ca^{2+} extrusion by Na^+–Ca^{2+} exchange (NCX) (Despa *et al.* 2002) leading to an increase in cytosolic $[Ca^{2+}]$ ($[Ca^{2+}]_i$). High diastolic $[Ca^{2+}]_i$ by itself can increase RyR activity and SR Ca^{2+} leak; however, the modulation of SR Ca^{2+} leak by $[Ca^{2+}]_i$ has not been characterized in detail.

The RyR (type 2) mediates most of diastolic SR Ca^{2+} leak in ventricular myocytes (Neary *et al.* 2002; Shannon *et al.* 2002; Zima *et al.* 2010). The majority of RyRs localize in the junctional SR where they form clusters of 10–200 channels (Franzini-Armstrong *et al.* 1999). Each of these subcellular microdomains constitutes an SR Ca^{2+} release unit (Cheng & Lederer, 2008). The simultaneous activation of RyRs within the release unit generates a locally restricted increase in $[Ca^{2+}]_i$, or Ca^{2+} spark (Cheng *et al.* 1993; Lopez-Lopez *et al.* 1995). After the discovery of Ca^{2+} sparks, it has been suggested that the entire diastolic SR Ca^{2+} leak can be explained solely by these spontaneous release events (Cheng *et al.* 1993; Bassani & Bers, 1995). However, this concept has been recently challenged. It has been reported that in ventricular myocytes a significant portion of SR Ca^{2+} leak occurs as undetectable openings of single RyRs or spark-independent Ca^{2+} leak (Santiago *et al.* 2010; Zima *et al.* 2010; Brochet *et al.* 2011; Porta *et al.* 2011). RyR-mediated SR Ca^{2+} leak strongly depends on intra-SR free Ca^{2+} ($[Ca^{2+}]_{SR}$). At low $[Ca^{2+}]_{SR}$, SR Ca^{2+} leak is mainly mediated by spark-independent pathways. At higher $[Ca^{2+}]_{SR}$, however, Ca^{2+} sparks become a significant contributor to SR Ca^{2+} leak (Zima *et al.* 2010). In certain pathological conditions associated with SR Ca^{2+} overload, SR Ca^{2+} leak becomes exacerbated. The Ca^{2+} released during a spontaneous spark diffuses to neighbouring release junctions, triggers CICR and generates arrhythmogenic spontaneous Ca^{2+} waves (Cheng *et al.* 1993; Diaz *et al.* 1997). While the importance of $[Ca^{2+}]_{SR}$ in the regulation of SR Ca^{2+} leak is well established, it is less clear to what extent $[Ca^{2+}]_i$ affects the RyR-mediated Ca^{2+} leak (Dibb & Eisner, 2010). $[Ca^{2+}]_i$ can regulate SR Ca^{2+} leak directly by binding to the high-affinity activation site on the cytosolic side of the RyR (Rousseau *et al.* 1986; Meissner & Henderson, 1987). Additionally, $[Ca^{2+}]_i$ can affect SR Ca^{2+} leak via activation of CaMKII with subsequent phosphorylation of the RyR (Guo *et al.* 2006; van Oort *et al.* 2010).

In our previous study, we investigated the effect of $[Ca^{2+}]_{SR}$ on SR Ca^{2+} leak (Zima *et al.* 2010) in conditions where $[Ca^{2+}]_i$ was held constant. In physiological conditions, however, $[Ca^{2+}]_i$ changes dynamically during the cardiac cycle. Therefore, it is important to understand to what extent $[Ca^{2+}]_i$ affects SR Ca^{2+} leak in ventricular myocytes. In this study, we used a novel approach to directly measure SR Ca^{2+} leak as changes of $[Ca^{2+}]_{SR}$ after complete SERCA inhibition. To measure $[Ca^{2+}]_{SR}$, we used the low-affinity Ca^{2+} indicator Fluo-5N entrapped within the SR. SR Ca^{2+} leak was studied after sarcolemma permeabilization. The advantage of this approach is that an experimental solution with known $[Ca^{2+}]$ can be easily introduced into the cytosol. The experimental solution also contained the high-affinity Ca^{2+} indicator Rhod-2 to measure Ca^{2+} spark and wave properties. We found that in rabbit ventricular myocytes $[Ca^{2+}]_i$ has a pronounced effect on SR Ca^{2+} leak. The augmentation of SR Ca^{2+} leak by $[Ca^{2+}]_i$ was attributed to an increase in both spark- and non-spark-mediated Ca^{2+} leak. The effect of $[Ca^{2+}]_i$ (within the range of 50–350 nM) on SR Ca^{2+} leak was mainly mediated by a direct regulation of RyR activity, but not by CaMKII-dependent phosphorylation of the RyR. Part of this work has been published in abstract form (Bovo *et al.* 2010).

Methods

Myocyte isolation

Ventricular myocytes were isolated from New Zealand White rabbits (18 animals, 2–2.5 kg; Myrtle's Rabbitry, Thompsons Station, TN, USA). The procedure of cell isolation was approved by the Institutional Animal Care and Use Committee, and complies with US and UK regulations on animal experimentation (Drummond, 2009). Adult rabbits were anaesthetized with sodium pentobarbital (50 mg kg^{-1} I.V.). Following thoracotomy, hearts were quickly excised, mounted on a Langendorff apparatus and retrogradely perfused with Liberase (Roche Applied Science, Indianapolis, IN, USA) Blendzyme (Roche Applied Science, Indianapolis, IN, USA)-containing solution at 37°C according to the procedure described previously (Domeier *et al.* 2009). Chemicals and reagents were purchased from Sigma-Aldrich (St Louis, MO, USA) unless otherwise stated. All experiments were performed at room temperature (20–24°C).

Confocal microscopy

To record $[Ca^{2+}]_{SR}$ and $[Ca^{2+}]_i$ we used the low-affinity Ca^{2+} indicator Fluo-5N and the high-affinity Ca^{2+} indicator Rhod-2, respectively (both indicators were obtained from Molecular Probes/Invitrogen, Carlsbad, CA, USA). To load the SR with Ca^{2+} indicator, myocytes were incubated with 5 μM Fluo-5N-AM for 2.5 h at 37°C as described previously (Zima *et al.* 2008*b*; Domeier *et al.* 2009).

For premeabilized cell experiments, Fluo-5N-AM-loaded myocytes were permeabilized with 0.005% saponin (Zima *et al.* 2008*a*). The experimental solution containing Rhod-2 tripotassium salt (40 μM) was composed of (in mM): potassium aspartate 100; KCl 15; KH_2PO_4 5; MgATP 5; EGTA 0.35; $CaCl_2$ 0.067; $MgCl_2$ 0.75; phosphocreatine 10; Hepes 10; plus creatine phosphokinase 5 U ml^{-1}; dextran (MW: 40,000) 4%, and pH 7.2 (KOH). Free $[Ca^{2+}]$ and $[Mg^{2+}]$ of this solution were 50 nM and 1 mM, respectively. Free $[Ca^{2+}]$ in the experimental solution was adjusted to different levels (i.e. 150, 250 and 350 nM) by adding appropriate amounts of $CaCl_2$ (calculated using WinMAXC 2.05, Stanford University, CA, USA). In the set of experiments when effects of increased cytosolic Ca^{2+} buffer capacity on Ca^{2+} sparks and SR Ca^{2+} leak were studied, the fast Ca^{2+} buffer BAPTA (0.7 mM) was added to the experimental solution. Free $[Ca^{2+}]$ in this solution was kept the same as the control solution (verified with a Ca^{2+}-sensitive electrode; Orion Research Inc.).

For intact cell experiments, Fluo-5N-AM-loaded cells were incubated at room temperature with 10 μM Rhod-2-AM for 15 min in Tyrode solution (in mM: NaCl 140; KCl 4; $CaCl_2$ 2; $MgCl_2$ 1; glucose 10; Hepes 10; pH 7.4), followed by a 20 min wash. Action potentials were induced by electrical field stimulation using a pair of platinum electrodes, which were connected to a Grass stimulator (Astro-Med. Inc., USA) set at a voltage ~50% above the threshold for contraction. To avoid motion artifacts, the scan line was positioned along the short axis (transversal scan) in the central region of the cell where cell motion is minimal during contraction. Stimulation frequency was 0.5 Hz. Changes in $[Ca^{2+}]_{SR}$ were calculated by the formula (Cannell *et al.* 1994): $[Ca^{2+}]_{SR} = K_d \times R/(K_d/[Ca^{2+}]_{SR,diast} - R + 1)$, where R was the normalized Fluo-5N fluorescence ($R = [F - F_{min}]/[F_0 - F_{min}]$); F_0 and F_{min} were the fluorescence level at rest and after depletion of the SR with caffeine, respectively; K_d (Fluo-5N Ca^{2+} dissociation constant) was 390 μM based on *in situ* calibrations (Zima *et al.* 2010), and $[Ca^{2+}]_{SR,diast}$ (diastolic $[Ca^{2+}]_{SR}$ at 0.5 Hz) was 900 μM (Shannon *et al.* 2003). Changes in $[Ca^{2+}]_i$ were calculated according to a similar formula (Cannell *et al.* 1994). K_d for Rhod-2 was 1.3 μM (calibrated *in situ*) and $[Ca^{2+}]_{i,diast}$ (diastolic $[Ca^{2+}]_i$ at 0.5 Hz) was 100 nM.

Changes in $[Ca^{2+}]_i$ and $[Ca^{2+}]_{SR}$ were measured with laser scanning confocal microscopy (Radiance 2000 MP, Bio-Rad, UK or LSM 410, Zeiss, Germany) equipped with a ×40 oil-immersion objective lens (NA = 1.3). Fluo-5N was excited with the 488 nm line of an argon ion laser and fluorescence was measured at 515 ± 15 nm. Rhod-2 was excited with the 543 nm line of a He–Ne laser and fluorescence was measured at wavelengths >600 nm. In experiments when Ca^{2+} sparks or global cytosolic Ca^{2+} transients were recorded simultaneously with $[Ca^{2+}]_{SR}$, images were acquired in line-scan mode (3 ms per scan; pixel size 0.12 μm). When $[Ca^{2+}]_{SR}$ was recorded alone (only Fluo-5N signal), images were collected in 2-D mode (pixel size 0.2 μm) every 15 s.

Measurements of SR Ca^{2+} leak

SR Ca^{2+} leak as a function of $[Ca^{2+}]_{SR}$ was measured in permeabilized myocytes according to the protocol described previously (Zima *et al.* 2010). Briefly, Fluo-5N was excited with minimum laser energy of an argon ion laser (to minimize dye photobleaching). To improve the signal-to-noise ratio of the low-intensity Fluo-5N signal, fluorescence was collected with an open pinhole and averaged over the entire cellular width of a line-scan or 2-D image. At the end of each experiment, minimum (F_{min}) and maximum (F_{max}) Fluo-5N fluorescence were estimated as we described previously (Zima *et al.* 2010). F_{min} was measured after depletion of the SR with 10 mM caffeine in the presence of 5 mM EGTA. F_{max} was measured following an increase of $[Ca^{2+}]$ to 10 mM in the presence of caffeine. Caffeine keeps RyRs open allowing $[Ca^{2+}]$ equilibration across the SR membrane (Shannon *et al.* 2003). The Fluo-5N signal was converted to $[Ca^{2+}]$

using the formula: $[Ca^{2+}]_{SR} = K_d \times (F - F_{min})/(F_{max} - F)$, where K_d was 390 μM. SR Ca^{2+} leak was measured as the changes of total $[Ca^{2+}]_{SR}$ ($[Ca^{2+}]_{SRT}$) over time ($d[Ca^{2+}]_{SRT}/dt$) after complete SERCA inhibition with thapsigargin (TG). $[Ca^{2+}]_{SRT}$ was calculated as: $[Ca^{2+}]_{SRT} = B_{max}/(1+K_d/[Ca^{2+}]_{SR}) + [Ca^{2+}]_{SR}$; where B_{max} (the total concentration of SR Ca buffer) and K_d were 2700 μM and 630 μM, respectively (Shannon *et al.* 2000). The rate of SR Ca^{2+} leak ($d[Ca^{2+}]_{SRT}/dt$) was plotted as a function of $[Ca^{2+}]_{SR}$ for each time point (15 s) during $[Ca^{2+}]_{SR}$ decline.

Measurements of Ca^{2+} sparks and waves

Ca^{2+} sparks were detected and analysed using SparkMaster (Picht *et al.* 2007). To exclude false-positive events, the threshold criterion for spark detection was 3.8. At this threshold no events were detected when SR Ca^{2+} was emptied after simultaneous application of caffeine (10 mM) and TG (10 μM). Analysis of Ca^{2+} sparks included spark frequency (sparks s^{-1} (100 $\mu m)^{-1}$), amplitude ($\Delta F/F_0$), full duration at half-maximal amplitude (FDHM; ms) and full width at half-maximal amplitude (FWHM; μm). F_0 is the initial fluorescence recorded under steady-state conditions and $\Delta F = F - F_0$. Ca^{2+} waves were measured in line-scan mode and analysed in terms of amplitude, frequency and propagation velocity.

Statistics

Data are presented as mean ± SEM of n measured cells. Statistical comparisons between groups were performed with Student's t test. Differences were considered statistically significant at $P < 0.05$.

Results

The effect of cytosolic $[Ca^{2+}]$ on SR Ca^{2+} leak

Effects of different $[Ca^{2+}]_i$ on SR Ca^{2+} leak were studied in permeabilized rabbit ventricular myocytes. SR Ca^{2+} leak was measured as the rate of $[Ca^{2+}]_{SR}$ decline after complete SERCA inhibition with thapsigargin (TG). Figure 1*A* shows representative examples of $[Ca^{2+}]_{SR}$ recordings in control conditions and after application of TG (10 μM). The recordings were made in different cells at $[Ca^{2+}]_i$ of 50, 150, 250 and 350 nM. An increase of $[Ca^{2+}]_i$ (applied at $t = 0$) augmented the initial $[Ca^{2+}]_{SR}$ (measured before TG application). On average, initial $[Ca^{2+}]_{SR}$ in the presence of 50, 150, 250 and 350 nM $[Ca^{2+}]_i$ were 759 ± 28 μM ($n = 11$), 765 ± 25 μM ($n = 21$;

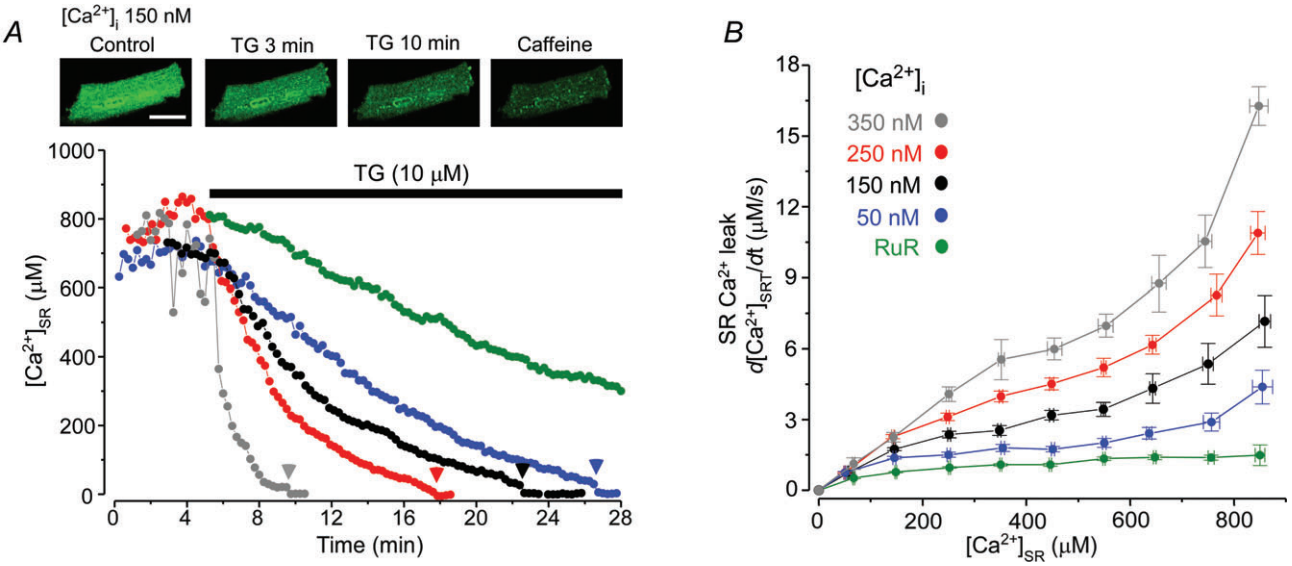

Figure 1. SR Ca^{2+} leak at different $[Ca^{2+}]_i$ values
A, changes of $[Ca^{2+}]_{SR}$ after inhibition of SERCA with thapsigargin (TG; 10 μM). Top, images of myocyte loaded with Fluo-5N in control conditions, after application of TG (10 μM; 3 and 10 min) and caffeine (10 mM). Calibration bar corresponds to 20 μm. Bottom, myocytes were exposed to different $[Ca^{2+}]_i$ values: 50 nM, blue; 150 nM, black; 250 nM, red; 350 nM, grey; and 150 nM in the presence of the RyR inhibitor Ruthenium Red (RuR; 50 μM), green. Since RyR inhibition with RuR significantly increases initial $[Ca^{2+}]_{SR}$ (Zima *et al.* 2010), for presentation purposes $[Ca^{2+}]_{SR}$ decline in the presence of RuR is shown from $[Ca^{2+}]_{SR} = 800$ μM to make it comparable with the other recordings. Application of 10 mM caffeine at the end of the experiment (arrowheads) indicates complete depletion of the SR. The recordings were made from different cells. *B*, relationships between SR Ca^{2+} leak rate and $[Ca^{2+}]_{SR}$ measured at different $[Ca^{2+}]_i$ values. SR Ca^{2+} leak was measured after inhibition of SERCA pump with TG.

NS compared to 50 nM); 828 ± 38 μM ($n = 16$; $P > 0.05$ compared to 50 nM) and 830 ± 44 μM ($n = 8$; $P > 0.05$ compared to 50 nM), respectively. These results suggest that higher $[Ca^{2+}]_i$ has a more significant effect on SERCA-mediated Ca^{2+} uptake than on SR Ca^{2+} leak. At 350 nM $[Ca^{2+}]_i$, initial $[Ca^{2+}]_{SR}$ frequently dropped below basal level as a result of the occurrence of Ca^{2+} waves.

After SERCA inhibition with TG, $[Ca^{2+}]_{SR}$ gradually declined until full depletion (verified as a lack of further $[Ca^{2+}]_{SR}$ depletion after caffeine application; arrowheads in Fig. 1*A*). $[Ca^{2+}]_{SR}$ after SERCA inhibition was converted to total $[Ca^{2+}]_{SR}$ ($[Ca^{2+}]_{SRT}$; for details see Methods). SR Ca^{2+} leak rate, which was measured as changes of $[Ca^{2+}]_{SRT}$ over time ($d[Ca^{2+}]_{SRT}/dt$), was plotted against the corresponding free $[Ca^{2+}]_{SR}$ to obtain the relationship between SR Ca^{2+} leak rate and $[Ca^{2+}]_{SR}$. The leak–load relationships measured in the presence of different $[Ca^{2+}]_i$ values are shown in Fig. 1*B*. SR Ca^{2+} leak significantly increased over the entire range of $[Ca^{2+}]_{SR}$ with increasing $[Ca^{2+}]_i$. To test whether $[Ca^{2+}]_i$ affected SR Ca^{2+} leak by activating RyRs, we studied effects of different $[Ca^{2+}]_i$ values on SR Ca^{2+} leak after complete RyR inhibition with ruthenium red (RuR). Figure 1*A* (green symbols) shows an example of $[Ca^{2+}]_{SR}$ decline in the presence of RuR (50 μM) and 150 nM $[Ca^{2+}]_i$. RuR significantly decreased SR Ca^{2+} leak, but did not prevent it (Fig. 1*B*). When RuR was applied at different $[Ca^{2+}]_i$ values, the rate of the RuR-insensitive Ca^{2+} leak remained the same (data not shown). Thus, these results indicate that $[Ca^{2+}]_i$ affects SR Ca^{2+} leak solely by modulating RyR activity.

Effects of cytosolic $[Ca^{2+}]$ on Ca^{2+} sparks and Ca^{2+} waves

For all $[Ca^{2+}]_i$ values studied here, SR Ca^{2+} leak increased as a function of $[Ca^{2+}]_{SR}$, with a particularly steep increase at higher $[Ca^{2+}]_{SR}$ (Fig. 1*B*). We have shown previously that the increased leak rate at higher $[Ca^{2+}]_{SR}$ is attributed to higher Ca^{2+} spark frequency (Zima *et al.* 2010). Here, we studied the effects of $[Ca^{2+}]_i$ on Ca^{2+} spark properties. Since $[Ca^{2+}]_{SR}$ increased as a function of $[Ca^{2+}]_i$ (Fig. 1*A*), we analysed the effect of changing $[Ca^{2+}]_i$ between 50 and 250 nM in a subset of cells that had similar $[Ca^{2+}]_{SR}$. Figure 2*A* shows representative line-scan images of SR Ca^{2+} release events recorded at different $[Ca^{2+}]_i$ values. The increase of $[Ca^{2+}]_i$ from 50 to 250 nM had a pronounced effect on spark frequency (Fig. 2*B*), which increased 5-fold. Ca^{2+} spark amplitude decreased (Fig. 2*C*), whereas spark width

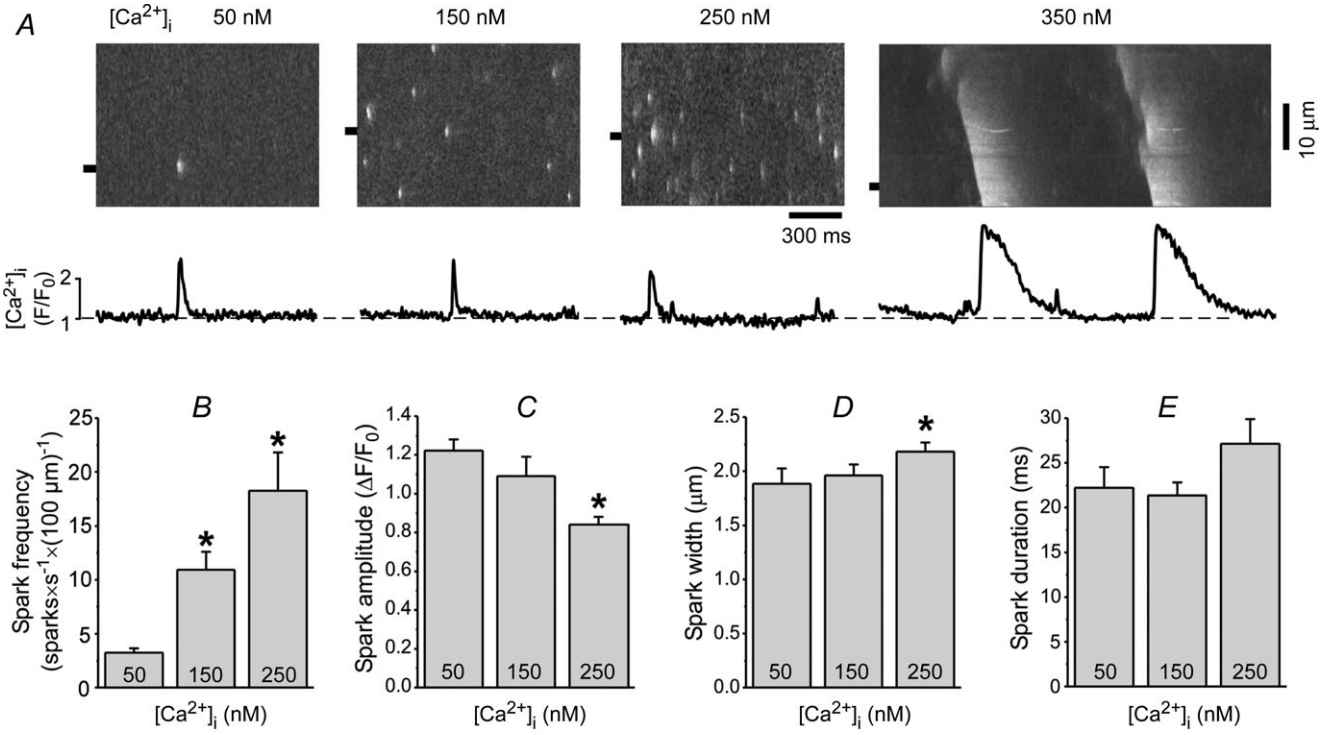

Figure 2. Effects of $[Ca^{2+}]_i$ on Ca^{2+} sparks and Ca^{2+} waves
A, example line-scan images and F/F_0 profiles of Ca^{2+} sparks and waves recorded at different $[Ca^{2+}]_i$ values. The Ca^{2+} spark and wave profiles were obtained by averaging fluorescence from the 1 μm wide region marked by the black boxes. Summary data of Ca^{2+} spark frequency (*B*), amplitude (*C*), width (measured at half-maximal amplitude, FWHM) (*D*), and duration (measured at half-maximal amplitude, FDHM) (*E*) recorded at different $[Ca]^{2+}_i$ values. *$P < 0.05$ *vs.* 50 nM $[Ca^{2+}]_i$.

(Fig. 2*D*) and duration (Fig. 2*E*) only slightly increased at higher $[Ca^{2+}]_i$. Increasing $[Ca^{2+}]_i$ to 350 nM produced spontaneous Ca^{2+} waves that propagated through the cell at a constant frequency of 0.9 ± 0.2 Hz ($n = 6$; Fig. 2*A*, rightmost image). These data indicate that $[Ca^{2+}]_i$ affects SR Ca^{2+} release and, therefore, spark-mediated SR Ca^{2+} leak. This occurs mainly via recruitment of the SR Ca^{2+} release units (spark frequency), but not via a profound alteration of release unit properties (spark width and duration).

Contribution of Ca^{2+} sparks and waves to SR Ca^{2+} leak at different cytosolic $[Ca^{2+}]$ values

We have recently shown that in rabbit ventricular myocytes RyR-mediated Ca^{2+} leak is composed of two main pathways: spark mediated and non-spark mediated (Zima *et al.* 2010). Depending on SR Ca^{2+} load, these two pathways contribute to a different degree to the total SR Ca^{2+} leak. At low $[Ca^{2+}]_{SR}$ (<400 μM), Ca^{2+} leak occurred mostly as undetectable openings of RyRs. At high $[Ca^{2+}]_{SR}$ (>600 μM), however, Ca^{2+} sparks became the significant pathway of SR Ca^{2+} leak. Here, we studied to what degree $[Ca^{2+}]_i$ affects these two components of SR Ca^{2+} leak. First, we obtained RyR-dependent Ca^{2+} leak as a function of $[Ca^{2+}]_{SR}$ (Fig. 3*A*) by subtracting the RuR-insensitive component of Ca^{2+} leak (Fig. 1*B*; green points) from the total SR Ca^{2+} leak (Fig. 1*B*). After subtraction, the points of SR Ca^{2+} leak at low $[Ca^{2+}]_{SR}$ (between 50 and 450 μM) were best fitted with single Hill functions (Fig. 3*B*) (Zima *et al.* 2010). These functions were used to describe the relationship between $[Ca^{2+}]_{SR}$ and non-spark-mediated Ca^{2+} leak for different $[Ca^{2+}]_i$

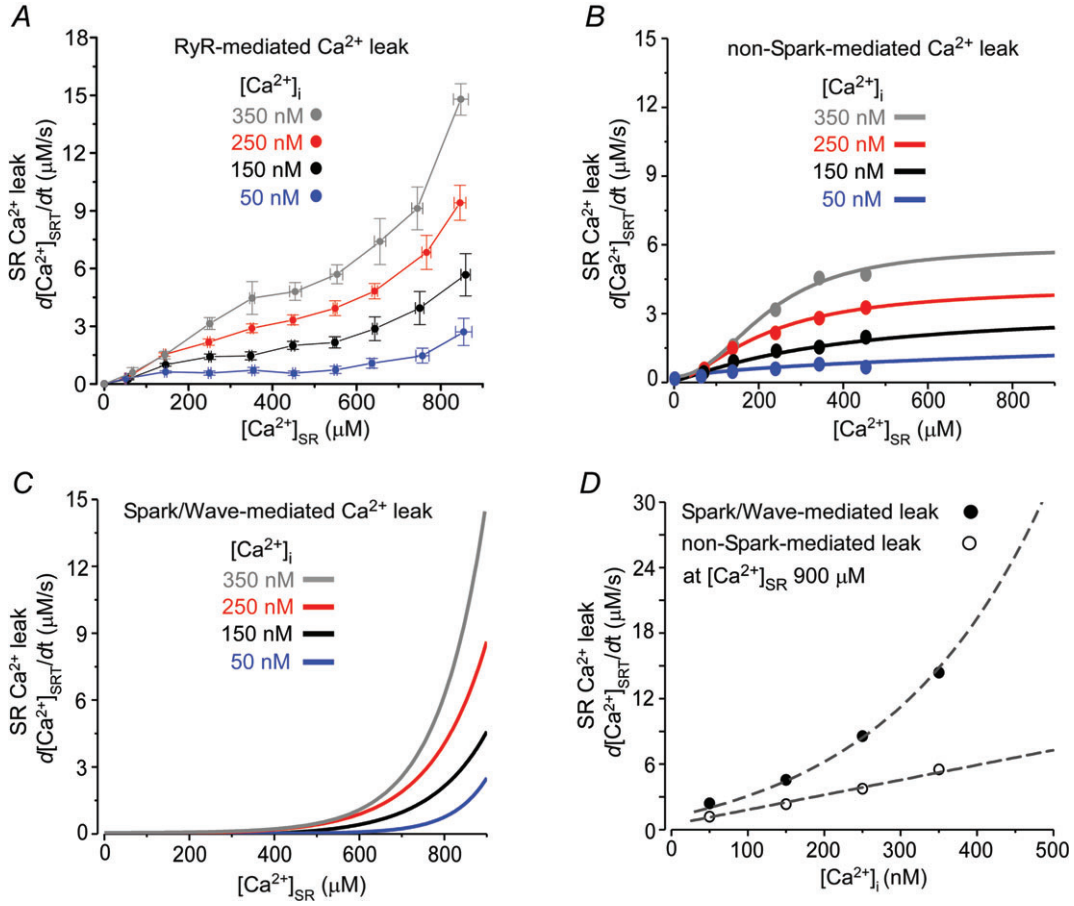

Figure 3. Contribution of Ca^{2+} sparks and waves to SR Ca^{2+} leak
A, RyR-mediated SR Ca^{2+} leak as a function of $[Ca^{2+}]_{SR}$ measured at different $[Ca^{2+}]_i$ values. The RyR-mediated Ca^{2+} leak was obtained by subtracting SR Ca^{2+} leak in the presence of RuR from the total SR Ca^{2+} leak. *B*, relationships between non-spark-mediated Ca^{2+} leak and $[Ca^{2+}]_{SR}$ obtained at different $[Ca]_i$ values. *C*, relationships between spark- and wave-mediated Ca^{2+} leak and $[Ca^{2+}]_{SR}$ obtained at different $[Ca]_i$ values. *D*, the spark-mediated Ca^{2+} leak (filled circles) and the non-spark mediated Ca^{2+} leak (open circles) at $[Ca^{2+}]_{SR} = 900$ μM were plotted as a function of $[Ca^{2+}]_i$. The spark-mediated leak was fitted with an exponential function ($R^2 = 0.86$) and the non-spark-mediated leak was fitted with a linear function ($R^2 = 0.91$).

values. Next, we estimated the spark-mediated leak by subtracting the corresponding non-spark-mediated leak (Fig. 3*B*) from the RyR-mediated Ca^{2+} leak (Fig. 3*A*). For different $[Ca^{2+}]_i$, the obtained points were best fitted with single exponential functions shown in Fig. 3*C*. In the case of 350 nM $[Ca^{2+}]_i$ (grey line), SR Ca^{2+} leak was mainly mediated by Ca^{2+} waves. Figure 3*D* illustrates the relative contribution of spark- and non-spark-mediated Ca^{2+} leak to the RyR-dependent Ca^{2+} leak (at $[Ca^{2+}]_{SR} = 900\ \mu M$) for different $[Ca^{2+}]_i$ values. This analysis revealed that both components of RyR-mediated Ca^{2+} leak increased as a function of $[Ca^{2+}]_i$. While non-spark-mediated Ca^{2+} leak increased linearly, spark/wave-mediated leak rose exponentially with $[Ca^{2+}]_i$. These results indicate that cytosolic $[Ca^{2+}]$ significantly affects both components of RyR-mediated Ca^{2+} leak in ventricular myocytes.

In the next set of experiments, we used the fast Ca^{2+} buffer BAPTA to eliminate Ca^{2+} sparks by decreasing efficacy of local CICR within RyR clusters. Addition of 0.7 mM BAPTA to the experimental solution decreased Ca^{2+} spark frequency by 87% (Fig. 4*A* and *B*), amplitude by 67% and width by 40%. Free $[Ca^{2+}]_i$ of the BAPTA solution was kept the same as the control solution (250 nM). As BAPTA did not affect basal $[Ca^{2+}]_{SR}$ (Fig. 4*C*), changes in spark properties were not due to decreased SR Ca^{2+} load. Therefore, by using BAPTA we were able to significantly eliminate spark-mediated Ca^{2+} leak without affecting single RyR activity. The analysis of SR Ca^{2+} leak at 250 nM $[Ca^{2+}]_i$ in the control solution and in the presence of BAPTA (0.7 mM) (Fig. 4*C*) revealed that an increase of cytosolic Ca^{2+} buffer capacity with BAPTA significantly decreased SR Ca^{2+} leak, particularly at high $[Ca^{2+}]_{SR}$ (>400 μM; Fig. 4*D*) where Ca^{2+} sparks significantly contribute to SR Ca^{2+} leak (Zima *et al.* 2010). Furthermore, Ca^{2+} leak measured in the presence of BAPTA was similar to non-spark-mediated Ca^{2+} leak obtained by the mathematical approach (Fig. 3*B* and dashed line in Fig. 4*D*).

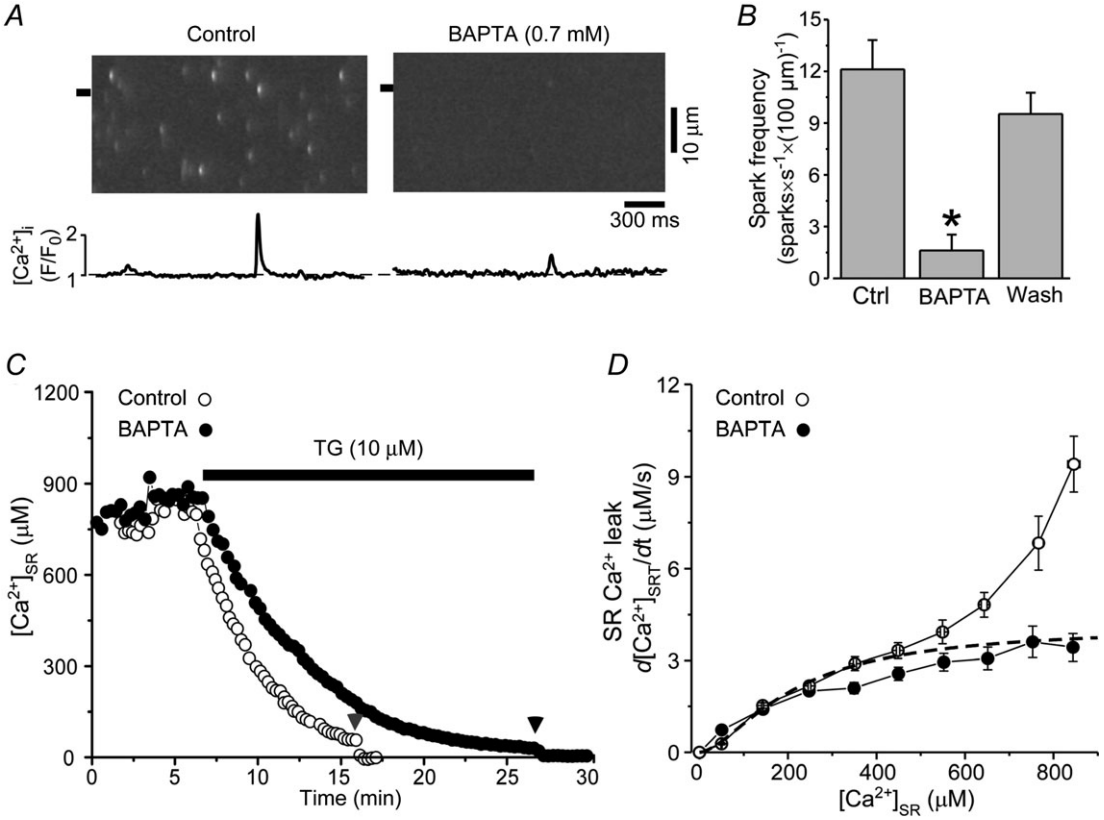

Figure 4. Effects of BAPTA on Ca^{2+} sparks and SR Ca^{2+} leak
A, line-scan images and F/F_0 profiles of Ca^{2+} sparks recorded at 250 nM $[Ca]_i$ in control and in the presence of 0.7 mM BAPTA. The Ca^{2+} spark profiles were obtained by averaging fluorescence from the 1 μm wide regions marked by the black boxes. *B*, effect of BAPTA on Ca^{2+} spark frequency. *C*, decline of $[Ca^{2+}]_{SR}$ during SERCA inhibition in control solution (open circles) and in the presence of 0.7 mM BAPTA (filled circles). Free $[Ca^{2+}]_i$ of both solutions was kept at 250 nM. *D*, relationships between SR Ca^{2+} leak and $[Ca^{2+}]_{SR}$ measured at 250 nM $[Ca^{2+}]_i$ in control (open circles) and BAPTA-containing solution (filled circles). For comparison, the dashed line indicates non-spark-mediated Ca^{2+} leak at 250 nM $[Ca^{2+}]_i$ obtained by the mathematical approach (data from Fig. 3*B*).

Role of CaMKII in regulation of SR Ca^{2+} leak at high cytosolic $[Ca^{2+}]$

In the following experiments, we investigated whether the augmentation of SR Ca^{2+} leak observed at high cytosolic $[Ca^{2+}]$ (>150 nM) was in part mediated by CaMKII-dependent phosphorylation of the RyR. Here we studied the effect of the specific CaMKII inhibitor autocamtide 2-related inhibitory peptide (AIP) on SR Ca^{2+} leak at high $[Ca^{2+}]_i$. Figure 5*A* shows a representative recording of $[Ca^{2+}]_{SR}$ in the presence of AIP (5 μM), after subsequently increasing $[Ca^{2+}]_i$ to 250 nM, as well as after application of TG (10 μM). AIP did not significantly affect initial $[Ca^{2+}]_{SR}$ (recorded before TG application). Initial $[Ca^{2+}]_{SR}$ was 795 ± 44 μM in control conditions and remained steady at 771 ± 66 μM ($n = 10$) after AIP application. In the presence of AIP, SR Ca^{2+} leak only changed from 7.2 ± 0.6 to 8.5 ± 1.1 μM s^{-1} ($n = 10$; $[Ca^{2+}]_{SR} = 750$ μM). Thus, inhibition of CaMKII did not have a significant effect on SR Ca^{2+} leak (Fig. 5*B*), although the results show a tendency to increase SR Ca^{2+} leak (~16%) at 250 nM $[Ca^{2+}]_i$. Likewise, we did not observe a significant effect of AIP on SR Ca^{2+} leak in the presence of 350 nM $[Ca^{2+}]_i$. SR Ca^{2+} leak was 16.0 ± 0.9 μM s^{-1} ($n = 8$) in control conditions and changed to 17.8 ± 1.4 μM s^{-1} ($n = 7$) after AIP (5 μM) application. AIP also did not change the properties of Ca^{2+} waves (i.e. frequency, amplitude and velocity; data not shown). These results indicate that CaMKII-mediated RyR phosphorylation is not involved in the effect of $[Ca^{2+}]_i$ (in the range from 50 to 350 nM) on SR Ca^{2+} leak. Thus, $[Ca^{2+}]_i$ regulates Ca^{2+} leak mainly via direct action on the RyR.

Changes of SR Ca^{2+} leak during excitation–contraction coupling (ECC)

RyR-mediated Ca^{2+} leak is controlled by the level of Ca^{2+} on both sides of the SR membrane (Fig. 1*B*). During the cardiac cycle, cytosolic and luminal $[Ca^{2+}]$ dynamically change, following opposite directions ($[Ca^{2+}]_{SR}$ is replenished while $[Ca^{2+}]_i$ declines and *vice versa*). Thus, the decline of $[Ca^{2+}]_i$ during late systole and early diastole would ultimately offset the stimulatory effect of $[Ca^{2+}]_{SR}$ on the RyR. In the following experiments, we measured changes of $[Ca^{2+}]_{SR}$ and $[Ca^{2+}]_i$ during ECC and analysed how these changes would affect SR Ca^{2+} leak. $[Ca^{2+}]_{SR}$ and $[Ca^{2+}]_i$ were recorded simultaneously in intact ventricular myocytes at 0.5 Hz pacing frequency. Figure 6*A* shows line-scan images of Ca^{2+} transient (top) and corresponding $[Ca^{2+}]_{SR}$ depletion (bottom) evoked by electrical field stimulation. We measured $[Ca^{2+}]_{SR}$ during a SR replenishing phase at the same three $[Ca^{2+}]_i$ values (150, 250 and 350 nM), that were studied in permeabilized cell experiments. $[Ca^{2+}]_i$ was inversely proportional to $[Ca^{2+}]_{SR}$ with a slope constant of –1100 (Fig. 6*B*). We estimated how changes in $[Ca^{2+}]_i$ and $[Ca^{2+}]_{SR}$ (which occur during diastole) affect SR Ca^{2+} leak. At 350 nM $[Ca^{2+}]_i$, $[Ca^{2+}]_{SR}$ was 608±45 μM ($n = 9$; Fig. 6*B*) and SR Ca^{2+} leak was 7.9 μM s^{-1} (Fig. 5*C*, blue open circle). At 250 nM $[Ca^{2+}]_i$, $[Ca^{2+}]_{SR}$ was replenished to 718 ± 27 μM ($n = 9$; Fig. 6*B*) and Ca^{2+} leak slightly decreased to 7.5 μM s^{-1} (Fig. 6*C*, red open circle). At 150 nM $[Ca^{2+}]_i$, $[Ca^{2+}]_{SR}$ reached 819 ± 11 μM ($n = 9$; Fig. 6*B*) and SR Ca^{2+} leak was further reduced to 6.9 μM s^{-1} (Fig. 6*C*, black open circle). This analysis suggests that only small changes (~13%) of SR Ca^{2+} leak occur during the declining phase

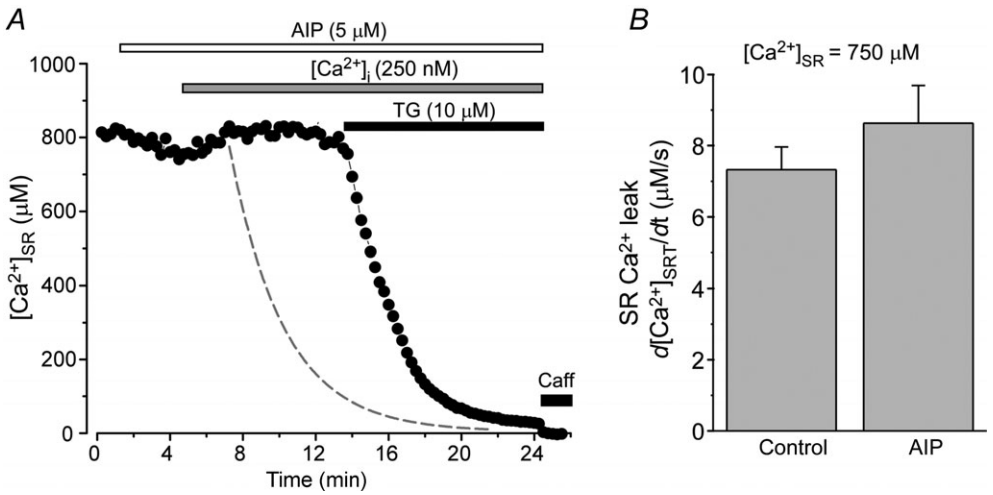

Figure 5. Effects of CaMKII inhibition on SR Ca^{2+} leak
A, effect of 250 nM $[Ca^{2+}]_i$ on decline of $[Ca^{2+}]_{SR}$ during SERCA inhibition in the presence of AIP (5 μM). For comparison, the dashed line indicates the decline of $[Ca^{2+}]_{SR}$ at 250 nM $[Ca^{2+}]_i$ in the absence of CaMKII inhibition (data from Fig. 1*A*). *B*, average effect of AIP (5 μM) on SR Ca^{2+} leak measured at $[Ca^{2+}]_{SR} = 750$ μM.

of the Ca^{2+} transient. Since SR Ca^{2+} leak steeply depends on both $[Ca^{2+}]_{SR}$ and $[Ca^{2+}]_i$ (Fig. 1*B*), but $[Ca^{2+}]_{SR}$ and $[Ca^{2+}]_i$ (Fig. 6*A*) change in opposite directions, SR Ca^{2+} leak remains relatively constant during the SR replenishing phase of the cardiac cycle.

Discussion

In recent years, a significant effort has been made to understand the mechanisms that control SR Ca^{2+} leak in healthy and diseased hearts. A relatively small augmentation of SR Ca^{2+} efflux during diastole can significantly influence cardiac function by depleting the SR Ca^{2+} content and reducing contraction. The increased Ca^{2+} leak can also be pro-arrhythmic as the released Ca^{2+} is extruded by the electrogenic Na^+–Ca^{2+} exchange (NCX), leading to delayed afterdepolarizations (Kass *et al.* 1978; Pogwizd *et al.* 2001). The bulk of SR Ca^{2+} leak is mediated by RyRs (Neary *et al.* 2002; Shannon *et al.* 2002; Zima *et al.* 2010), which are complexly regulated by Ca^{2+} from both cytosolic and luminal sides of the channel (Fill & Copello, 2002; Meissner, 2004). Since Fabiato's work (Fabiato, 1985*a*,*b*), $[Ca^{2+}]_i$ has been considered a crucial factor in the activation of global SR Ca^{2+} release during systole. However, it is less clear to what extent dynamic changes of $[Ca^{2+}]_i$ during diastole affects RyR activity and SR Ca^{2+} leak. Here we directly measured Ca^{2+} leak as the rate of $[Ca^{2+}]_{SR}$ decline after SERCA inhibition in permeabilized rabbit ventricular myocytes. By introducing different $[Ca^{2+}]_i$ levels into the cytosol, we found that: (1) $[Ca^{2+}]_i$ increases SR Ca^{2+} leak primarily by activating the RyR-mediated leak pathway; (2) with increasing $[Ca^{2+}]_i$, Ca^{2+} sparks and waves become significant pathways of Ca^{2+} leak; (3) within the range of 50–350 nM $[Ca^{2+}]_i$, the effect on SR Ca^{2+} leak is predominantly mediated by direct activation of the RyR and not by CaMKII-mediated phosphorylation of the channel; and (4) during late systole and early diastole (when $[Ca^{2+}]_{SR}$ and $[Ca^{2+}]_i$ change in opposite directions) SR Ca^{2+} leak remains relatively constant as a result of strong dependence from both $[Ca^{2+}]_i$ and $[Ca^{2+}]_{SR}$.

Our results show that $[Ca^{2+}]_i$ affects SR Ca^{2+} leak entirely by regulating RyR activity. We found that in the presence of the potent RyR inhibitor RuR, the residual SR Ca^{2+} leak was insensitive to changes in $[Ca^{2+}]_i$. High $[Ca^{2+}]_i$ can facilitate SR Ca^{2+} leak by increasing RyR open probability. However, it also decreases the SR Ca^{2+} gradient and therefore the driving force for SR Ca^{2+} leak. Our results show that despite decrease of the SR Ca^{2+} gradient (by changing $[Ca^{2+}]_i$ from 50 to 350 nM), RyR-mediated Ca^{2+} leak increased more than 5 times (measured at the same $[Ca^{2+}]_{SR}$; Figs 1*B* and 3*A*). This finding suggests that SR Ca^{2+} leak is not a simple diffusion of Ca^{2+} from the SR, but rather a well-regulated process. We have previously shown that RyR-mediated Ca^{2+} leak can occur as spontaneous Ca^{2+} sparks, but also as undetectable openings of RyRs (non-spark-mediated Ca^{2+} leak; Zima *et al.* 2010). The augmentation of SR Ca^{2+} leak by cytosolic Ca^{2+} was attributed to an increase of both components of SR Ca^{2+} leak (Fig. 3*B* and *C*). These two pathways, however, were differently regulated

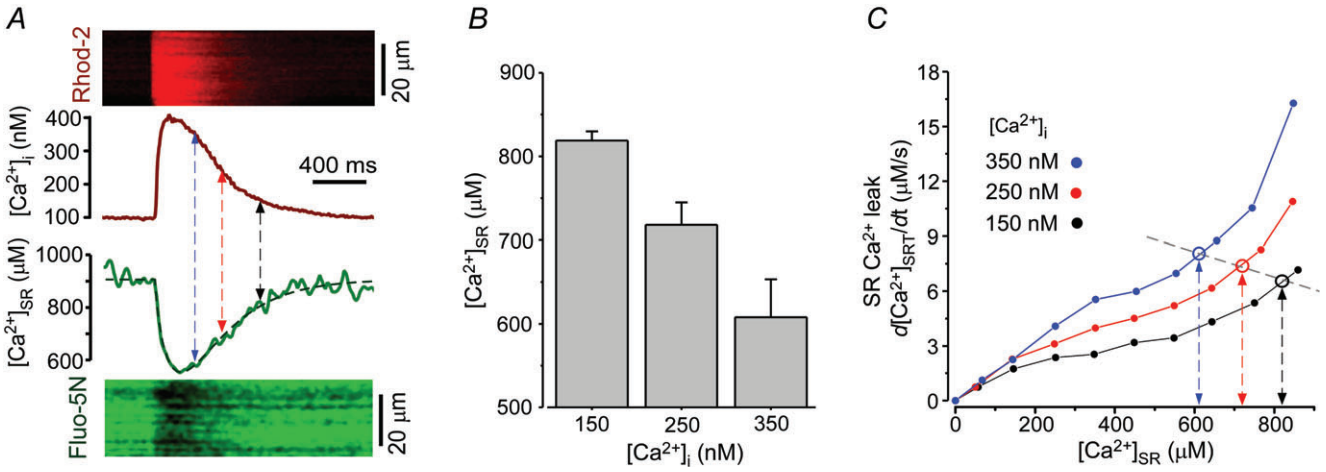

Figure 6. Estimation of SR Ca^{2+} leak during the declining phase of the Ca^{2+} transient
A, simultaneously recorded $[Ca^{2+}]_i$ transient and corresponding $[Ca^{2+}]_{SR}$ depletion. Top, line-scan image of Rhod-2 fluorescence and profile of $[Ca^{2+}]_i$. Bottom, line-scan image of Fluo-5N fluorescence and profile of $[Ca^{2+}]_{SR}$. The profiles were obtained by averaging fluorescence from the entire cellular width of line scans. *B*, summary data showing changes of $[Ca^{2+}]_{SR}$ measured at three different $[Ca^{2+}]_i$ values (i.e. 150, 250 and 350 nM; indicated by arrows in *A*). *C*, RyR-mediated SR Ca^{2+} leak as a function of $[Ca^{2+}]_{SR}$ measured at different $[Ca^{2+}]_i$ values (data were taken from Fig. 3*A*). For each $[Ca^{2+}]_i$ studied, SR Ca^{2+} leak was extrapolated at the corresponding $[Ca^{2+}]_{SR}$, calculated from the $[Ca^{2+}]_{SR}$ profile in *A*. The results suggest that during the declining phase of the Ca^{2+} transient leak remains relatively constant.

by $[Ca^{2+}]_i$. While non-spark-mediated Ca^{2+} leak linearly depended on $[Ca^{2+}]_i$ (Fig. 3*D*), spark-mediated Ca^{2+} leak rose steeply at higher $[Ca^{2+}]_i$. The latter was mainly mediated by an increase of Ca^{2+} spark frequency, since other spark properties (width and duration) were only minimally affected by $[Ca^{2+}]_i$ (Fig. 2). A similar effect of $[Ca^{2+}]_i$ on spark frequency was observed in permeabilized rat ventricular myocytes (Lukyanenko & Gyorke, 1999).

The analysis of the spark properties also shows that the amplitude proportionally decreased with an increase of $[Ca^{2+}]_i$, indicating that this spark parameter is mainly determined by SR Ca^{2+} release flux and, therefore, by the SR Ca^{2+} gradient. However, despite the Ca^{2+} flux during individual release events at 350 nM $[Ca^{2+}]_i$ being smaller than at $[Ca^{2+}]_i < 350$ nM, it is sufficient to increase $[Ca^{2+}]_i$ next to neighbouring junctions to activate local CICR and trigger Ca^{2+} waves. When $[Ca^{2+}]_{SR}$ was depleted to $\sim$500 μM (during SERCA inhibition) Ca^{2+} waves ceased completely (data not shown), suggesting that the $[Ca^{2+}]$ on both sides of the RyR plays an important role in the generation of Ca^{2+} waves. It appears that high $[Ca^{2+}]_i$ increases the sensitivity of release units to CICR and elevated $[Ca^{2+}]_{SR}$ maintains SR Ca^{2+} flux strong enough to produce Ca^{2+} waves via a 'fire–diffuse–fire' mechanism (Keizer & Smith, 1998). We found that the transformation of SR Ca^{2+} release from localized sparks to propagating waves almost doubled RyR-mediated Ca^{2+} leak (Fig. 3*C*), suggesting that Ca^{2+} waves represent spontaneous SR Ca^{2+} release events in their extreme form.

It has been suggested that an increase of SR Ca^{2+} leak by high $[Ca^{2+}]_i$ is mediated partially by CaMKII-dependent phosphorylation of RyRs (Guo *et al.* 2006; van Oort *et al.* 2010). Using the selective CaMKII inhibitor AIP, we found that the augmentation of SR Ca^{2+} leak at high $[Ca^{2+}]_i$ was insensitive to CaMKII inhibition. In contrast to previous studies, AIP treatment showed some tendency to accelerate SR Ca^{2+} leak (Fig. 5). The discrepancy with previously published work can be explained by the fact that CaMKII was not activated under our experimental conditions. It has been shown that activation of endogenous CaMKII requires much higher $[Ca^{2+}]_i$ ($\sim$500 nM), phosphatase inhibition (e.g. with okadaic acid) and calmodulin (Guo *et al.* 2006). In our experiments none of these conditions were applied. The small acceleration of SR Ca^{2+} leak observed in the presence of AIP can be the result of a potential direct interaction of the peptide with the RyR. Thus, in the range of 50–350 nM $[Ca^{2+}]_i$ regulates SR Ca^{2+} leak mainly via a CaMKII-independent mechanism.

Another important finding of this study is that SR Ca^{2+} leak is highly sensitive to both $[Ca^{2+}]_i$ and $[Ca^{2+}]_{SR}$ (Fig. 1*B*). It remains unresolved whether luminal and cytosolic Ca^{2+} regulate the RyR via entirely independent mechanisms or via a well coordinated process. It has been shown that the RyR can be activated independently by Ca^{2+} from the luminal or cytosolic sides of the channel (Sitsapesan & Williams, 1994; Gyorke & Gyorke, 1998; Qin *et al.* 2008). However, luminal $[Ca^{2+}]$ can also regulate RyR by acting on the cytosolic Ca^{2+} activation site of the channel via a 'feed-through' mechanism (Laver, 2007). The combination of all these regulatory mechanisms contributes to the fine control of the RyR. Furthermore, our data suggest that $[Ca^{2+}]_{SR}$ regulation provides an important feedback mechanism to counter the positive feedback of high $[Ca^{2+}]_i$ during the declining phase of the Ca^{2+} transient, whereas at the end of diastole, the high SR Ca^{2+} leak driving force determined by high $[Ca^{2+}]_{SR}$ is well equilibrated by the low $[Ca^{2+}]_i$. The balance established by this dual regulation results in a SR Ca^{2+} leak rate that remains relatively constant during the decline of the Ca^{2+} transient when $[Ca^{2+}]_{SR}$ and $[Ca^{2+}]_i$ change in opposite directions. However, alterations in the activity of RyR during diastole can affect the basal Ca^{2+} leak rate and, therefore, the amount of Ca^{2+} stored in the SR. This would lead to altered systolic Ca^{2+} transients, potential generation of arrhythmias and contractile dysfunctions. There are, however, significant differences between animal species regarding the role of RyR modification and its effect on SR Ca^{2+} release and ECC. In rat ventricular myocytes, for example, RyR sensitization with low doses of caffeine produced only a transient positive inotropic effect (Trafford *et al.* 2000). However, studies conducted on ventricular myocytes from larger animals (e.g. dogs and rabbits) (Belevych *et al.* 2007; Domeier *et al.* 2009) showed that caffeine led to significant depletion of $[Ca^{2+}]_{SR}$ and a decrease of Ca^{2+} transient amplitude. The differences between rats and rabbits are probably due to the differences in expression of SERCA and NCX (Bers, 2001). In contrast to rats, rabbits have less SERCA but increased NCX expression. This translates functionally into less SR Ca^{2+} reuptake by SERCA, more Ca^{2+} extrusion from the cell via NCX, and greater net cellular Ca^{2+} loss.

The coordinated regulation of RyR by luminal and cytosolic Ca^{2+} provides a fundamental mechanism that contributes to setting the appropriate SR Ca^{2+} load during diastole and therefore preventing the onset of pathological conditions (e.g. SR Ca^{2+} overload). This is an important step towards the understanding of the RyR regulation. In intact cells, however, additional mechanisms are probably involved. For instance, our estimation did not account for a potential SR Ca^{2+} release refractoriness which can occur during ECC in intact cells. In permeabilized cells, the potential contribution of Ca^{2+}-dependent inactivation (Fabiato, 1985*b*) in offsetting the SR Ca^{2+} leak at high $[Ca^{2+}]_i$ can be ruled out based on several previous findings. First, Ca^{2+}-dependent inactivation has not been reported in permeabilized cell experiments when SR Ca^{2+} release was measured at $[Ca^{2+}]_i > 10$ μM (Stevens *et al.* 2009). Second, the study of cardiac RyR in lipid bilayers has shown that RyR inactivation occurs at significantly higher $[Ca^{2+}]_i$ (>0.5 mM) (Xu *et al.* 1996). Thus, the 13%

difference between the leak rates at the different points of $[Ca^{2+}]_i$ and corresponding $[Ca^{2+}]_{SR}$ during the declining phase of the Ca^{2+} transient (Fig. 6*C*), might be explained by the fact that our estimations obtained in permeabilized cells are not accounting for all the regulatory mechanisms that play a role in setting the RyR activity in the intact cellular environment (e.g. use-dependent inactivation).

In conclusion, this study is the first that we know of to characterize the effect of $[Ca^{2+}]_i$ on SR Ca^{2+} leak in permeabilized ventricular myocytes. We found that $[Ca^{2+}]_i$ plays a critical role in controlling SR Ca^{2+} leak. The increase of $[Ca^{2+}]_i$ and RyR sensitivity to $[Ca^{2+}]_i$ in heart failure or other pathological conditions, can lead to the alteration of diastolic SR Ca^{2+} leak and to the generation of arrhythmogenic events. These findings are of great importance because they explain a new regulatory mechanism of SR Ca^{2+} leak that is critical to maintain the physiological homeostasis of Ca^{2+} in the heart.

References

Ai X, Curran JW, Shannon TR, Bers DM & Pogwizd SM (2005). Ca^{2+}/calmodulin-dependent protein kinase modulates cardiac ryanodine receptor phosphorylation and sarcoplasmic reticulum Ca^{2+} leak in heart failure. *Circ Res* **97**, 1314–1322.

Bassani RA & Bers DM (1995). Rate of diastolic Ca release from the sarcoplasmic reticulum of intact rabbit and rat ventricular myocytes. *Biophys J* **68**, 2015–2022.

Belevych A, Kubalova Z, Terentyev D, Hamlin RL, Carnes CA & Gyorke S (2007). Enhanced ryanodine receptor-mediated calcium leak determines reduced sarcoplasmic reticulum calcium content in chronic canine heart failure. *Biophys J* **93**, 4083–4092.

Bers DM (2001). *Excitation-Contraction Coupling and Cardiac Contractile Force*. Kluwer Academic Publishers, Dordrecht.

Bers DM, Eisner DA & Valdivia HH (2003). Sarcoplasmic reticulum Ca^{2+} and heart failure: roles of diastolic leak and Ca^{2+} transport. *Circ Res* **93**, 487–490.

Bovo E, Blatter LA & Zima AV (2010). Regulation of sarcoplasmic reticulum calcium leak by cytosolic calcium in rabbit ventricular myocytes. *Biophys J* **98**, 102a.

Brochet DX, Xie W, Yang D, Cheng H & Lederer WJ (2011). Quarky calcium release in the heart. *Circ Res* **108**, 210–218.

Cannell MB, Cheng H & Lederer WJ (1994). Spatial non-uniformities in $[Ca^{2+}]_i$ during excitation-contraction coupling in cardiac myocytes. *Biophys J* **67**, 1942–1956.

Cheng H & Lederer WJ (2008). Calcium sparks. *Physiol Rev* **88**, 1491–1545.

Cheng H, Lederer WJ & Cannell MB (1993). Calcium sparks: elementary events underlying excitation-contraction coupling in heart muscle. *Science* **262**, 740–744.

Despa S, Islam MA, Weber CR, Pogwizd SM & Bers DM (2002). Intracellular Na^+ concentration is elevated in heart failure but Na/K pump function is unchanged. *Circulation* **105**, 2543–2548.

Diaz ME, Trafford AW, O'Neill SC & Eisner DA (1997). Measurement of sarcoplasmic reticulum Ca^{2+} content and sarcolemmal Ca^{2+} fluxes in isolated rat ventricular myocytes during spontaneous Ca^{2+} release. *J Physiol* **501**, 3–16.

Dibb K & Eisner D (2010). A small leak may sink a great ship but what does it do to the heart? *J Physiol* **588**, 4849.

Domeier TL, Blatter LA & Zima AV (2009). Alteration of sarcoplasmic reticulum Ca^{2+} release termination by ryanodine receptor sensitization and in heart failure. *J Physiol* **587**, 5197–5209.

Drummond GB (2009). Reporting ethical matters in *The Journal of Physiology*: standards and advice. *J Physiol* **587**, 713–719.

Fabiato A (1983). Calcium-induced release of calcium from the cardiac sarcoplasmic reticulum. *Am J Physiol Cell Physiol* **245**, C1–C14.

Fabiato A (1985*a*). Rapid ionic modifications during the aequorin-detected calcium transient in a skinned canine cardiac Purkinje cell. *J Gen Physiol* **85**, 189–246.

Fabiato A (1985*b*). Time and calcium dependence of activation and inactivation of calcium-induced release of calcium from the sarcoplasmic reticulum of a skinned canine cardiac Purkinje cell. *J Gen Physiol* **85**, 247–289.

Fill M & Copello JA (2002). Ryanodine receptor calcium release channels. *Physiol Rev* **82**, 893–922.

Franzini-Armstrong C, Protasi F & Ramesh V (1999). Shape, size, and distribution of Ca^{2+} release units and couplons in skeletal and cardiac muscles. *Biophys J* **77**, 1528–1539.

George CH (2008). Sarcoplasmic reticulum Ca^{2+} leak in heart failure: mere observation or functional relevance? *Cardiovasc Res* **77**, 302–314.

Guo T, Zhang T, Mestril R & Bers DM (2006). Ca^{2+}/calmodulin-dependent protein kinase II phosphorylation of ryanodine receptor does affect calcium sparks in mouse ventricular myocytes. *Circ Res* **99**, 398–406.

Gyorke I & Gyorke S (1998). Regulation of the cardiac ryanodine receptor channel by luminal Ca^{2+} involves luminal Ca^{2+} sensing sites. *Biophys J* **75**, 2801–2810.

Jiang MT, Lokuta AJ, Farrell EF, Wolff MR, Haworth RA & Valdivia HH (2002). Abnormal Ca^{2+} release, but normal ryanodine receptors, in canine and human heart failure. *Circ Res* **91**, 1015–1022.

Kass RS, Lederer WJ, Tsien RW & Weingart R (1978). Role of calcium ions in transient inward currents and aftercontractions induced by strophanthidin in cardiac Purkinje fibres. *J Physiol* **281**, 187–208.

Keizer J & Smith GD (1998). Spark-to-wave transition: saltatory transmission of calcium waves in cardiac myocytes. *Biophys Chem* **72**, 87–100.

Laver DR (2007). Ca^{2+} stores regulate ryanodine receptor Ca^{2+} release channels via luminal and cytosolic Ca^{2+} sites. *Biophys J* **92**, 3541–3555.

Lehnart S & Marks AR (2007). Regulation of ryanodine receptors in the heart. *Circ Res* **101**, 746–749.

Lopez-Lopez JR, Shacklock PS, Balke CW & Wier WG (1995). Local calcium transients triggered by single L-type calcium channel currents in cardiac cells. *Science* **268**, 1042–1045.

Lukyanenko V & Gyorke S (1999). Ca^{2+} sparks and Ca^{2+} waves in saponin-permeabilized rat ventricular myocytes. *J Physiol* **521**, 575–585.

Marx SO, Reiken S, Hisamatsu Y, Jayaraman T, Burkhoff D, Rosemblit N & Marks AR (2000). PKA phosphorylation dissociates FKBP12.6 from the calcium release channel (ryanodine receptor): defective regulation in failing hearts. *Cell* **101**, 365–376.

Meissner G (2004). Molecular regulation of cardiac ryanodine receptor ion channel. *Cell Calcium* **35**, 621–628.

Meissner G & Henderson JS (1987). Rapid calcium release from cardiac sarcoplasmic reticulum vesicles is dependent on Ca^{2+} and is modulated by Mg^{2+}, adenine nucleotide, and calmodulin. *J Biol Chem* **262**, 3065–3073.

Neary P, Duncan AM, Cobbe SM & Smith GL (2002). Assessment of sarcoplasmic reticulum Ca^{2+} flux pathways in cardiomyocytes from rabbits with infarct-induced left-ventricular dysfunction. *Pflugers Arch* **444**, 360–371.

O'Rourke B, Kass DA, Tomaselli GF, Kaab S, Tunin R & Marban E (1999). Mechanisms of altered excitation-contraction coupling in canine tachycardia-induced heart failure, I: experimental studies. *Circ Res* **84**, 562–570.

Picht E, Zima AV, Blatter LA & Bers DM (2007). SparkMaster – automated calcium spark analysis with ImageJ. *Am J Physiol Cell Physiol* **293**, C1073–C1081.

Pieske B, Kretschmann B, Meyer M, Holubarsch C, Weirich J, Posival H *et al.* (1995). Alterations in intracellular calcium handling associated with the inverse force-frequency relation in human dilated cardiomyopathy. *Circulation* **92**, 1169–1178.

Pogwizd SM, Qi M, Yuan W, Samarel AM & Bers DM (1999). Upregulation of Na^+/Ca^{2+} exchanger expression and function in an arrhythmogenic rabbit model of heart failure. *Circ Res* **85**, 1009–1019.

Pogwizd SM, Schlotthauer K, Li L, Yuan W & Bers DM (2001). Arrhythmogenesis and contractile dysfunction in heart failure: Roles of sodium-calcium exchange, inward rectifier potassium current, and residual beta-adrenergic responsiveness. *Circ Res* **88**, 1159–1167.

Porta M, Zima AV, Nani A, Diaz-Sylvester PL, Copello JA, Ramos-Franco J *et al.* (2011). Single ryanodine receptor channel basis of caffeine's action on Ca^{2+} sparks. *Biophys J* **100**, 931–938.

Qin J, Valle G, Nani A, Nori A, Rizzi N, Priori SG *et al.* (2008). Luminal Ca^{2+} regulation of single cardiac ryanodine receptors: insights provided by calsequestrin and its mutants. *J Gen Physiol* **131**, 325–334.

Rousseau E, Smith JS, Henderson JS & Meissner G (1986). Single channel and $45Ca^{2+}$ flux measurements of the cardiac sarcoplasmic reticulum calcium channel. *Biophys J* **50**, 1009–1014.

Santiago DJ, Curran JW, Bers DM, Lederer WJ, Stern MD, Rios E & Shannon TR (2010). Ca sparks do not explain all ryanodine receptor-mediated SR Ca leak in mouse ventricular myocytes. *Biophys J* **98**, 2111–2120.

Shannon TR, Ginsburg KS & Bers DM (2000). Reverse mode of the sarcoplasmic reticulum calcium pump and load-dependent cytosolic calcium decline in voltage-clamped cardiac ventricular myocytes. *Biophys J* **78**, 322–333.

Shannon TR, Ginsburg KS & Bers DM (2002). Quantitative assessment of the SR Ca^{2+} leak-load relationship. *Circ Res* **91**, 594–600.

Shannon TR, Guo T & Bers DM (2003). Ca^{2+} scraps: local depletions of free $[Ca^{2+}]$ in cardiac sarcoplasmic reticulum during contractions leave substantial Ca^{2+} reserve. *Circ Res* **93**, 40–45.

Sitsapesan R & Williams AJ (1994). Regulation of the gating of the sheep cardiac sarcoplasmic reticulum Ca^{2+}-release channel by luminal Ca^{2+}. *J Membr Biol* **137**, 215–226.

Stevens SC, Terentyev D, Kalyanasundaram A, Periasamy M & Gyorke S (2009). Intra-sarcoplasmic reticulum Ca^{2+} oscillations are driven by dynamic regulation of ryanodine receptor function by luminal Ca^{2+} in cardiomyocytes. *J Physiol* **587**, 4863–4872.

Terentyev D, Gyorke I, Belevych AE, Terentyeva R, Sridhar A, Nishijima Y *et al.* (2008). Redox modification of ryanodine receptors contributes to sarcoplasmic reticulum Ca^{2+} leak in chronic heart failure. *Circ Res* **103**, 1466–1472.

Trafford AW, Sibbring GC, Diaz ME & Eisner DA (2000). The effects of low concentrations of caffeine on spontaneous Ca release in isolated rat ventricular myocytes. *Cell Calcium* **28**, 269–276.

van Oort RJ, McCauley MD, Dixit SS, Pereira L, Yang Y, Respress JL *et al.* (2010). Ryanodine receptor phosphorylation by calcium/calmodulin-dependent protein kinase II promotes life-threatening ventricular arrhythmias in mice with heart failure. *Circulation* **122**, 2669–2679.

Xu L, Mann G & Meissner G (1996). Regulation of cardiac Ca^{2+} release channel (ryanodine receptor) by Ca^{2+}, H^+, Mg^{2+}, and adenine nucleotides under normal and simulated ischemic conditions. *Circ Res* **79**, 1100–1109.

Zima AV, Bovo E, Bers DM & Blatter LA (2010). Ca^{2+} spark-dependent and -independent sarcoplasmic reticulum Ca^{2+} leak in normal and failing rabbit ventricular myocytes. *J Physiol* **588**, 4743–4757.

Zima AV, Picht E, Bers DM & Blatter LA (2008*a*). Partial inhibition of sarcoplasmic reticulum Ca release evokes long-lasting Ca release events in ventricular myocytes: role of luminal Ca in termination of Ca release. *Biophys J* **94**, 1867–1879.

Zima AV, Picht E, Bers DM & Blatter LA (2008*b*). Termination of cardiac Ca^{2+} sparks: role of intra-SR $[Ca^{2+}]$, release flux, and intra-SR Ca^{2+} diffusion. *Circ Res* **103**, e105–e115.

Author contributions

E.B., S.R.M., A.V.Z. and L.A.B. contributed to the conception and design of the study, interpretation of data and writing of the manuscript. E.B., S.R.M. and A.V.Z. performed the experimental work and analysis of results. All authors have approved the version to be published.

Acknowledgement

This work was supported by National Institutes of Health Grants HL62231, HL80101 and HL101235, the Leducq Foundation (to L.A.B.) and the McCormick Foundation (to A.V.Z.). The authors also would like to thank Drs Seth L. Robia and Joshua Maxwell for critical reading of the manuscript.